Directed self-organization of trenched templates for nanowire growth

Yan-Mei Yu[1,2,3,a)] and Axel Voigt[1,b)]
[1]*Institut für Wissenschaftliches Rechnen, Technische Universität Dresden, 01062 Dresden, Germany*
[2]*Institute of Physics, Chinese Academy of Sciences, P.O. Box 603, 100190 Beijing, People's Republic of China*
[3]*Beijing National Laboratory of Condensed Matter Physics, Beijing 100190, People's Republic of China*

(Received 5 November 2008; accepted 8 January 2009; published online 27 January 2009)

We combine a proposed approach to fabricate self-organized nanowires, which are grown in trenched templates, with a periodic strain field of a buried misfit dislocation network or a compliant substrate to guide the kinetic roughening and coarsening process in the formation of the template. Numerical simulations of the directed self-organization process show the possibility to form perfectly ordered parallel trenches with adjustable period, which allows to grow extended nanowires. © *2009 American Institute of Physics*. [DOI: 10.1063/1.3076112]

Bottom-up approaches can provide cost-efficient ways to produce nanowires by using self-organization of various chemical reactions.[1–3] The resulting nanowires are typically randomly arranged and thus not directly suitable for applications. To overcome these limitations the self-organization process needs to be guided. One way is to produce nanowires by step decoration of vicinal surfaces[4,5] with the arrangement of the nanowires depending on the step morphology. Besides steps also cracks are used as molds to be filled to form nanowires and thus the nanowire arrangement is directed by the regular crack network.[6] In Ref. 7 a simpler method is described to obtain ordered arrays of planar nanowires on flat commercial wafers. The method consists of first fabrication of a flat buffer layer, second a template displaying a uniaxial array of trenches, and third the layer-by-layer deposition at the bottom of the trenches to form the nanowires. It has been demonstrated that the process can be tailored to form magnetic nanowires with functionality at room temperature and adjustable magnetic properties that fulfill requirements for applications such as recording media, spin electronics, and logic devices.[8]

A key feature to produce nanowires using this method is the perfect ordering of the trenched templates. The described method uses a kinetic self-organization process, which occurs at metal bcc (110) surfaces as a result of an Ehrlich–Schwoebel (ES) barrier and an anisotropic attachment process. The early stage of such a growth mechanism has been verified by kinetic monte carlo (KMC) simulations.[9,10] Large scale simulations of the trench growth by phase-field models[11] reproduce qualitatively the experimentally observed trenches[7] and explain the kinetic self-organization process. Due to the ES barrier, mounds form and coarsen during growth. Due to the anisotropy, the coarsening is slow in one direction and fast in the other direction, which causes formation of the trench arrays at the early stage. At long time, the trench arrays develop the quasiperiodic uniaxial structure as a consequence of competition between coarsening and roughening for the selected transversal slope and the decreasing longitudinal slope. Figure 1 shows snapshots of such simulations. One key feature is the development of a stationary facet angle, which guarantees that the shape of the trenches is not influenced by fluctuations of their width.

However, even if the kinetic self-organization process is well understood and the period of the trenches is controllable, a perfect ordering of parallel trenches, which would be required for the applications mentioned above, could not yet be obtained with this approach, neither experimentally nor in simulations. The final ordering of the trenches depends sensitively on the nucleation of islands on the buffer layer. Therefore, we propose to modify the fabrication of a flat buffer layer in the first process in Ref. 7, such that in the second process the kinetic self-organization of the trenches can be directed by influencing the nucleation. Various methods[12–15] have been proposed toward directed self-organization of nanostructures, which use a periodic strain field of a buried misfit dislocation network or a compliant substrate to control sites for island nucleation. In particular the strain field alters the potential energy surface by modifying the transition and adsorption energy, as calculated for metals using density functional theory.[16] The difference of the two energies ΔE enters the rate of adatom surface diffusion $D=D_0 \exp(-\Delta E/k_B T)$.[17,18] In addition, the change in the adsorption energy generates a thermodynamic drift term for the adatoms. In Refs. 19 and 20 the level-set simulations have demonstrated that these effects cause the preferred

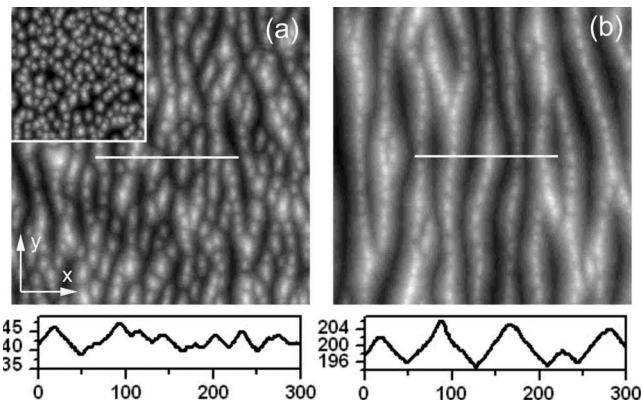

FIG. 1. Simulated trench morphology on W(110) after deposition of (a) 40 ML and (b) 200 ML, and cross-section profiles along the white line at the bottom. The image size is $650a \times 650a$ (i.e., 195×195 nm^2 of W surface with $a=0.3$ nm). Inset: morphology of nucleated islands after deposition of 2 ML in cut image of the same scale with the main image.

a)Electronic mail: yan-mei.yu@tu-dresden.de.
b)Electronic mail: axel.voigt@tu-dresden.de.

nucleation of islands in regions of fast diffusion or minimal adsorption energy, so that an ordered array of nucleated islands is achieved at the submonolayer regime. The modifications of the potential energy surface become small with the increase in the distance to the buried dislocations, and then the related effects is of importance only for small deposition coverages. According to the results of Ref. 19, we start with an array of submonolayer islands and simulate the subsequent formation and growth of trenches by using the phase field simulation.[21,22] Different from Ref. 19, we concentrate on the morphological evolution for larger deposition coverages. Besides, the strain-induced effects are not incorporated into the phase-field equations, instead considered through an initial condition of the periodic array of the submonolayer islands. The system to be solved reads

$$\partial_t \phi = \frac{1}{\tau(\theta)}[\nabla \cdot (W^2 \nabla \phi) - 2\sin(2\pi\phi) - 2\lambda(\cos(2\pi\phi) - 1)u] + \lambda_n u^{i+1} \quad (1)$$

$$\partial_t u = \nabla \cdot (D \nabla u) - \partial_t \phi + \Omega \delta(\vec{r} - \vec{r}')\delta(t - t'). \quad (2)$$

Thereby phase-field variable ϕ distinguishes atomic layers by using $\phi = 1, 2, 3, \ldots$, to describe the first, second, third, … monolayers starting from the buffer layer. The sharp steps between these layers are approximated through a diffuse interface of $\nabla\phi \neq 0$. The twofold anisotropy of atomic attachment kinetics on bcc(110) surface is formulated by $\tau(\theta) = \bar{\tau}[1 + \eta\cos(2\theta)]$, wherein θ is angle between normal to island boundary to x-coordinate, and τ reaches minimum at island boundary that is along x direction (where $\theta = 90°, 270°$), and maximum at island boundary that is along y direction (where $\theta = 0°, 360°$). The parameters W, $\bar{\tau}$, λ, and η of Eq. (1) are chosen to meet the material specific anisotropic step stiffness and the kinetic coefficient in the thin-interface limit.[11,23] The first term in Eq. (1) describes the step growth and the second term describes island nucleation, with i being a critical nucleation size and λ_n being a parameter of the nucleation kinetics. In Eq. (2) the adatom density u is described according to diffusion, consumption, and deposition of adatoms. The new adatoms are added at a point $\vec{r}'$ randomly every time interval that is determined by the deposition flux F.

For the simulations we choose parameters, which model $W(110)$ surfaces at $T = 553$ K and $F = 0.4$ ML/s using $\lambda_n = D$, $i = 2$, and $\eta = 0.6$. In the simulations the random deposition of adatoms in Eq. (2) indicates the random distribution of adatoms and then random nucleation according to the last term in Eq. (1). In Fig. 1 the initial condition is an open substrate where nucleated islands distributed randomly, as shown in the inset in Fig. 1(a), which leads to fluctuation of the width of the final trenches. In Fig. 2 we use a prescribed initial condition shown in the insets, where 50 submonolayer islands are set (i.e., $\phi = 1$) with random size, random location in each row, and the island rows are parallel with a certain period. Figure 2 shows surface morphology after deposition of 200 ML for the prescribed initial condition. The preferential island nucleation and growth is observed on the prescribed submonolayer islands, which forms parallel trenches by following the initial configuration. Depending on the period of the initial islands, perfectly aligned trenches can be observed. Within a certain parameter range the period of the trenches is controlled by the period of the islands and thus as a consequence the period of the buried dislocations.[19] The cross-section profiles in Fig. 2(d) indicates the uniform height, slope, and width of the trenches.

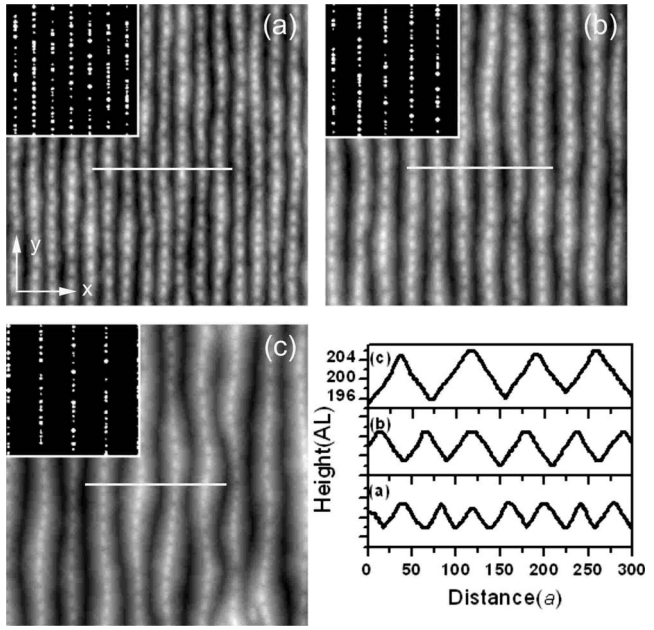

FIG. 2. Simulated trench morphology after deposition of 200 ML on a prescribed initial condition. Inset: cut image of the initial condition, periodic array of submonolayer island rows, of the same scale with main image. The main image size is $650a \times 650a$ (i.e., 195×195 nm^2 of W surface with $a = 0.3$ nm). In (a)–(c) the period of the initial island rows and the final trenches is 40, 56, and $70a$ (i.e., 12, 17, and 21 nm on W surface). (d) cross section along the white line.

We calculate the correlation length L_x and the slope S_x according to the global height-height correlation of these evolving morphologies. For the trench growth shown in Fig. 1, a typical coarsening is illustrated by $L_x \sim \vartheta^{0.22}$, as denoted by square in Fig. 3. Corresponding to Figs. 2(a) and 2(b), L_x stops by $40a$ and $56a$, as denoted by up-triangular and down-triangular in Fig. 3, being consistent to the prescribed initial period. As denoted by circle for $l = 70a$, the prephase coars-

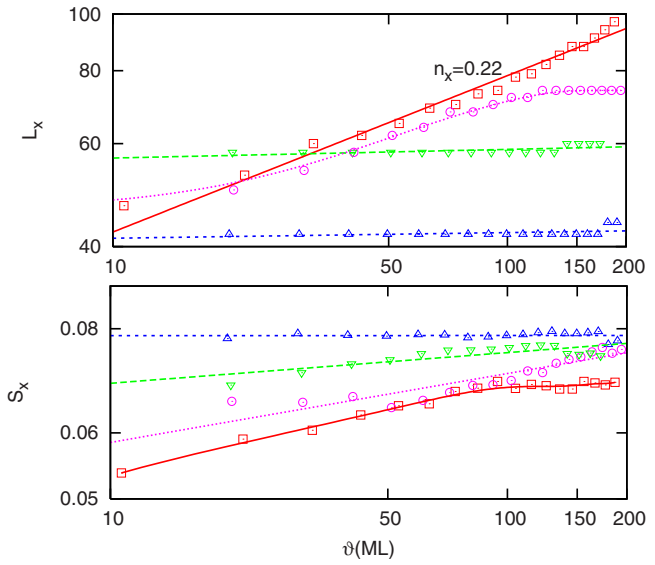

FIG. 3. (Color online) The evolution of the correlation length L_x and the slope S_x of the trenches vs the coverage-unpatterned (square), initial island period of $40a$ (up-triangular), $56a$ (down-triangular), and $70a$ (circle).

ening is caused by the island nucleation in between the prescribed submonolayer-island rows at the early stage. These islands are small and overwhelmed soon by the preferred growth on the prescribed sites, and then after $\vartheta > 150$ ML, L_x stops by $75a$, being close to the prescribed initial period, corresponding to the regular trenches in Fig. 2(c). The trenches form stationary side slopes, wherein S_x reaches a constant values after $\vartheta > 150$ ML in all cases, with a stationary value independent of the prescribed initial period.

In summary, preferential trench growth with prescribed period and guided growth dynamics can be achieved on prepatterned surfaces, resulting, e.g., from a buried misfit dislocation network. The preferential trench growth inherits the geometry of the ordered submonolayer islands, which leads to well separated trenches, which prevents coarsening among them, such that the ordered arrangement is maintained for long times. The simulations indicate that periodic arrangements of the submonolayer islands in the range of $30a < l < 100a$ lead to perfectly ordered trenches with adjustable period according to the initial period. For $l > 100a$, growth condition become similar to the unpatterned substrate, and for $l < 30a$, we observe fast coarsening and again similar behavior as for unpatterned substrates. In both limits the regular period of the final trenches is broken. Growth conditions determine the characteristic separation length among the islands, which in general is described as $l_s \sim D/F$. On prepatterned surface l_s is changed in terms of the prescribed space l. Thus smaller periods of trench arrays can be achieved by use of simulation condition that indicate smaller l_s, such as larger F. Likewise, larger periods of trench arrays require growth condition that indicate larger l_s, for example smaller F. The simulations support the development of a uniform trench size and side slope. Thereby the array period is designed by the period of submonolayer islands, resulting from a buried dislocation network, as described in Ref. 19. Our simulations thus suggest a possible pathway toward ordered growth of trenched template for self-organized fabrication of nanowires.

We would like to thank O. Fruchart and C. Ratsch for helpful discussions. A.V. and Y.M.Y. were supported by EU STRP 016447 and NSF DMR Award No. 0502737 within the project "MagDot." A.V. was supported by DFG through Grant No. Vo-899/7-1 and Y.M.Y. was supported by Chinese Department of Science and Technology (Grant No. 2005CB623602).

[1] T. Thurn-Albrecht, J. Schotter, G. A. Kastle, N. Emley, T. Shibauchi, L. Krusin-Elbaum, K. Guarini, C. T. Black, M. T. Tuominen, and T. P. Russell, Science **290**, 2126 (2000).
[2] M. P. Zach, K. H. Ng, and R. M. Penner, Science **290**, 2120 (2000).
[3] P. A. Smith, C. D. Nordquist, T. N. Jackson, T. S. Mayer, B. R. M. J. Mbindyo, and T. E. Mallouk, Appl. Phys. Lett. **77**, 1299 (2000).
[4] J. Hauschild, U. Gradmann, and H. J. Elmers, Appl. Phys. Lett. **72**, 3211 (1998).
[5] A. Dallmeyer, C. Carbone, W. Eberhardt, C. Pampuch, O. Rader, W. Gudat, P. Gambardella, and K. Kern, Phys. Rev. B **61**, R5133 (2000).
[6] B. E. Alaca, H. Sehitoglu, and T. Saif, Appl. Phys. Lett. **84**, 4669 (2004).
[7] B. Borca, O. Fruchart, P. David, A. Rousseau, and C. Meyer, Appl. Phys. Lett. **90**, 142507 (2007).
[8] D. A. Allwood, G. Xiong, C. C. Faulkner, D. Atkinson, D. Petit, and R. P. Cowburn, Science **309**, 1688 (2005).
[9] M. Albrecht, H. Fritzsche, and U. Gradmann, Surf. Sci. **294**, 1 (1993).
[10] C. Köhler, C. Jensen, C. Wolf, A. C. Schindler, L. Brendel, and D. E. Wolf, Surf. Sci. **454**, 676 (2000).
[11] Y.-M. Yu, R. Backofen, and A. Voigt, Phys. Rev. E **77**, 051605 (2008).
[12] A. E. Romanov, P. M. Petroff, and J. S. Speck, Appl. Phys. Lett. **74**, 2280 (1999).
[13] H. J. Kim, Z. M. Zhao, and Y. H. Xie, Phys. Rev. B **68**, 205312 (2003).
[14] S. M. Wise, J. S. Lowengrub, J. S. Kim, K. Thornton, P. W. Voorhees, and W. C. Johnson, Appl. Phys. Lett. **87**, 133102 (2005).
[15] E. Pan, M. Sun, P. W. Chung, and R. Zhu, Appl. Phys. Lett. **91**, 193110 (2007).
[16] C. Ratsch, A. P. Seitsonen, and M. Scheffler, Phys. Rev. B **55**, 6750 (1997).
[17] G. Russo and P. Smereka, J. Comput. Phys. **214**, 809 (2006).
[18] F. Haußer, M. Jabbour, and A. Voigt, Multiscale Model. Simul. **6**, 158 (2007).
[19] X. Niu, R. Vardavas, R. E. Caflisch, and C. Ratsch, Phys. Rev. B **74**, 193403 (2006).
[20] X. Niu, Y. Lee, R. E. Caflisch, and C. Ratsch, Phys. Rev. Lett. **101**, 086103 (2008).
[21] F. Otto, P. Penzler, A. Rätz, T. Rump and A. Voigt, Nonlinearity **17**, 477 (2004).
[22] Y. M. Yu and B. G. Liu, Phys. Rev. B **70**, 205414 (2004).
[23] A. Karma and W. J. Rappel, Phys. Rev. E **57**, 4323 (1998).